ACS APPLIED MATERIALS & INTERFACES

Letter

www.acsami.org

2D Perovskite Nanosheets with Thermally-Stable High-κ Response: A New Platform for High-Temperature Capacitors

Yoon-Hyun Kim,[†,‡] Hyung-Jun Kim,[†] Minoru Osada,*[,†,‡] Bao-Wen Li,[†] Yasuo Ebina,[†] and Takayoshi Sasaki[†]

[†]International Center for Materials Nanoarchitechtonics (WPI-MANA), National Institute for Materials Science (NIMS), Tsukuba 305-0044, Japan

[‡]Graduate School of Advanced Science and Engineering, Waseda University, Shinjyu-ku, Tokyo 169-8555, Japan

Supporting Information

ABSTRACT: We investigated high-temperature dielectric responses of high-κ perovskite nanosheet ($Ca_2Nb_3O_{10}$), an important material platform for postgraphene technology and ultrascale electronic devices. Through *in situ* characterizations using conducting atomic force microscopy, we found a robust high-temperature property of $Ca_2Nb_3O_{10}$ nanosheet even in a monolayer form (~2 nm). Furthermore, layer-by-layer assembled nanocapacitors retained both size-free high-ε_r characteristic (~200) and high insulation resistance (~1 × 10^{-7} A/cm^2) at high temperatures up to 250 °C. The simultaneous improvement of ε_r and thermal stability in high-κ nanodielectrics is of critical technological importance, and perovskite nanosheet has great potential for a rational design and construction of high-temperature capacitors.

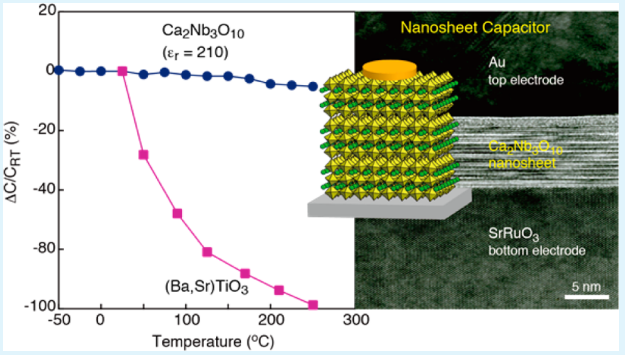

KEYWORDS: *2D perovskite nanosheet, nanodielectric, thermal stability, high-temperature capacitor, in situ characterization*

The search of new electronic materials for high-temperature applications has been a significant challenge in recent years.[1−3] In automotive industries, for example, cutting-edge technology requires electronic components operable at high temperatures (>200 °C). The absence of suitable capacitors is one of the major barriers to meet this goal. Capacitors are ubiquitous in electronic devices and systems. $BaTiO_3$ has been widely used in capacitor applications for many years. However, $BaTiO_3$ has a relatively low Curie temperature (T_C) of ~130 °C; a sharp decrease in ε_r above T_C intrinsically limits $BaTiO_3$-based materials for the use of high-temperature environments >200 °C. Various strategies have been made for tailoring the thermal stability of $BaTiO_3$ and related perovskites. In $BaTiO_3$, chemical modification by doping or solid solutions with other metal oxides is an effective approach to obtain a broadened dielectric peak while maintaining high permittivity (ε_r).[4−8] Another approach is the use of non-polar characteristic of layered ferroelectric materials having high T_C (e.g., $CaBi_4Ti_4O_{15}$, $SrBi_4Ti_4O_{15}$).[9,10] In future electronics, the requirements for capacitor devices generally tend toward miniaturized dielectrics with higher ε_r, lower loss, and reduced leakage current. The development of new high-temperature nanodielectrics to fulfill these requirements is an important issue but most challenging.

Here we provide a solution to these issues by using new high-κ nanosheet ($Ca_2Nb_3O_{10}$) with a paraelectric characteristic. Paraelectric materials (such as Al_2O_3, TiO_2) exhibit no ferroelectric hysteresis with a temperature-independent ε_r, ideal for high-temperature applications. However, these paraelectric materials usually possess low ε_r values (<100), and thus they have not been considered as a prime target for high-temperature capacitors. Recently we introduced a new material platform for high-κ dielectrics using two-dimensional (2D) oxide nanosheets derived from layered compounds by exfoliation.[11] Perovskite $Ca_2Nb_3O_{10}$ nanosheet (Figures 1a, 1b) is such an important target.[12] This nanosheet is a 2D single crystal with the thickness of ~1.5 nm, corresponding to three NbO_6 octahedra. Because the exfoliated nanosheets can extract the key functional blocks from their parent layered perovskites, the exfoliation and restacking processes of perovskite nanosheets would provide an ideal base for high-κ dielectrics with a critical thickness. The multilayer nanofilms of $Ca_2Nb_3O_{10}$ nanosheets realized the highest permittivity (ε_r = 210) of all known perovskite dielectrics in the ultrathin region (<10 nm).[12,13] One more important aspect of $Ca_2Nb_3O_{10}$ nanosheet is its thermal stability; 2D perovskite structure was stable up to 700 °C even in a monolayer film with an extremely small thickness of ~2 nm.[14] These features indicate that $Ca_2Nb_3O_{10}$ nanosheet is a very useful for the use of high-temperature

Received: September 27, 2014
Accepted: November 5, 2014
Published: November 5, 2014

   dx.doi.org/10.1021/am506629g | *ACS Appl. Mater. Interfaces* 2014, 6, 19510−19514

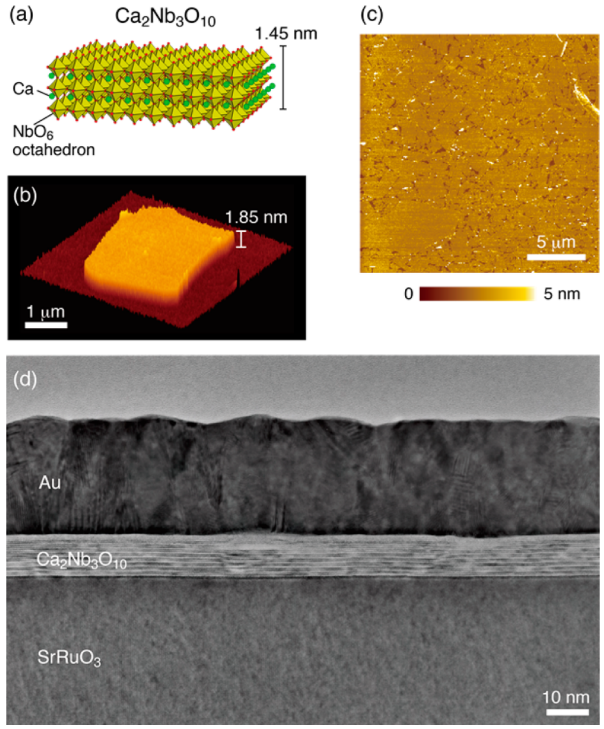

Figure 1. (a) Structure and (b) typical AFM image of a $Ca_2Nb_3O_{10}$ nanosheet. (c) AFM image for a monolayer LB film of $Ca_2Nb_3O_{10}$ nanosheets. (d) High-resolution TEM image of an Au/$(Ca_2Nb_3O_{10})_n$/$SrRuO_3$ nanocapacitor (n = 10).

capacitors. However, our previous study was *ex situ* experiments; the samples were prepared by high-temperature annealing at 400−900 °C, and the characterizations were carried out at room temperature. For true understanding of high-temperature properties of nanosheet-based capacitors, *in situ* characterization is highly required because it sheds new light on materials properties in the harsh environment for the use in practical devices.

In this study, we performed *in* situ high-temperature measurements of dielectric and insulating properties of $Ca_2Nb_3O_{10}$ nanosheets using atomic force microscopy (AFM) and micro prober technique. Through these *in situ* characterizations, we found a robust thermal stability of $Ca_2Nb_3O_{10}$ nanosheet even in a monolayer form (~2 nm), and layer-by-layer assembled nanocapacitors exhibited a stable temperature characteristic up to 250 °C, suitable for the use of high-density capacitors in high-temperature applications. Also, since *in situ* high-temperature dielectric property itself is quite rare for nanomaterials, our data of perovskite nanosheets offer an important experimental input for nanodielectrics and 2D materials.

A colloidal suspension of $Ca_2Nb_3O_{10}$ perovskite nanosheets was prepared by delaminating a layered perovskite ($KCa_2Nb_3O_{10}$) according to previously described procedures.[15] An atomically flat $SrRuO_3$ film, consisting of a 50 nm-thick (001)-oriented epitaxial $SrRuO_3$ film on a (001) $SrTiO_3$ single crystal, was used as a bottom electrode. To fabricate multilayer nanofilms, we used the Langmuir−Blodgett (LB) technique to perform layer-by-layer assembly.[16] The LB approach, combined with the use of an atomically flat $SrRuO_3$ substrate, is effective for room-temperature fabrication of an atomically uniform monolayer film with a highly dense characteristic (Figure 1c). Repeated LB deposition of the monolayer yielded multilayer nanofilms. These films were irradiated by UV white light from a Xe lamp (4 mW/cm^2) for 48 h in order to decompose tetrabuthylammonium hydroxide ions used in the exfoliation process. Electrical measurement was carried out by forming Au/$(Ca_2Nb_3O_{10})_n$/$SrRuO_3$ nanocapacitors (Figure 1d) (see experimental details in the Supporting Information). Complementary data were also obtained from *A*- and *B*-site modified nanosheets ($Sr_2Nb_3O_{10}$, $Ca_2Ta_3O_{10}$, $Sr_2Ta_3O_{10}$).

We first studied the insulating behavior of individual $Ca_2Nb_3O_{10}$ nanosheets by conducting AFM using environment controlled scanning probe microscopy (see experimental details in the Supporting Information). *In situ* AFM measurements of morphology and conducting maps were carried out at 25, 100, and 200 °C (Figure 2). For 25 °C (Figure 2b−d), $Ca_2Nb_3O_{10}$ nanosheet showed a highly insulating nature even in the 2 nm thick monolayer. From a comparison between morphology and conducting mapping (Figure 2c, d), the nanosheet interior exhibited a high resistance with current level of <10 pA, whereas a highly conducting behavior was observed in the

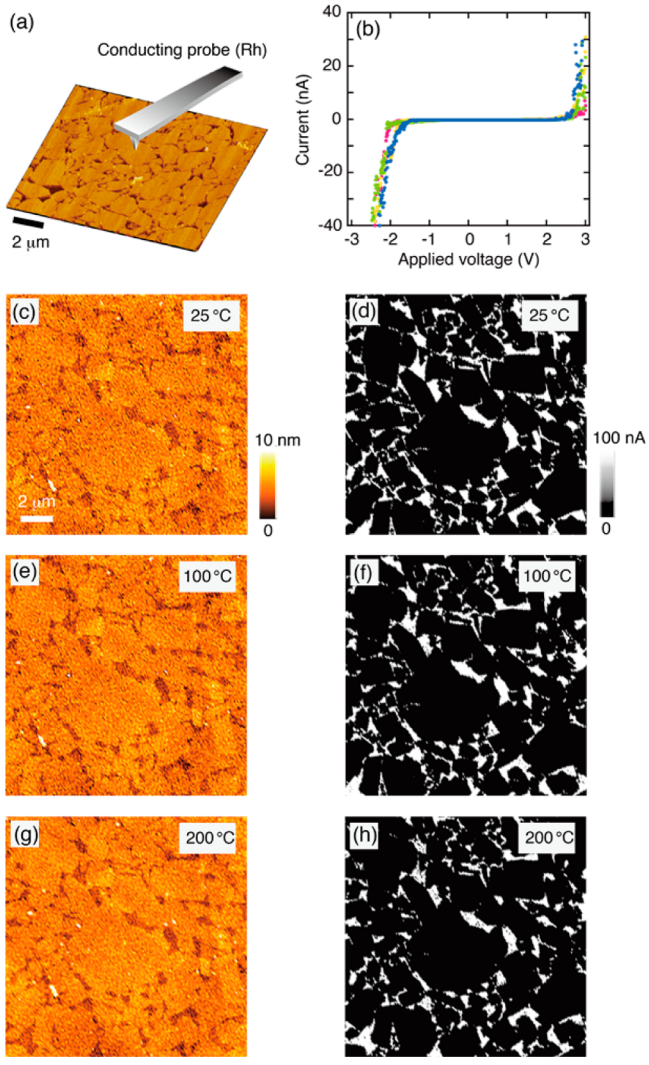

Figure 2. *In situ* high-temperature AFM of individual $Ca_2Nb_3O_{10}$ nanosheets. (a) Experimental setup for conducting AFM. (b) Typical I−V curves obtained from individual $Ca_2Nb_3O_{10}$ nanosheets on a $SrRuO_3$ substrate. (c−h) Topographic and conducting mapping images for a monolayer LB film of $Ca_2Nb_3O_{10}$ nanosheets on a $SrRuO_3$ substrate: (c, d) 25, (e, f) 100, and (g, h) 200 °C.

dx.doi.org/10.1021/am506629g | *ACS Appl. Mater. Interfaces* 2014, 6, 19510−19514

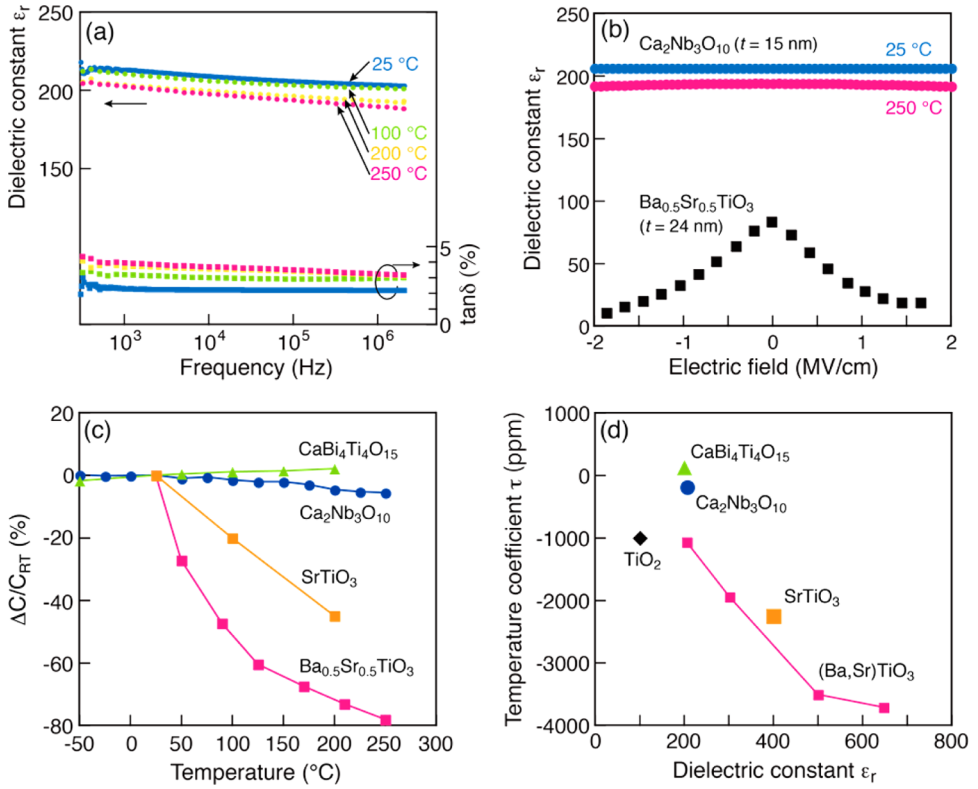

Figure 3. (a) Frequency dependence of the ε_r and tan δ of an Au/$(Ca_2Nb_3O_{10})_n$/$SrRuO_3$ (n = 10) nanocapacitor at 25, 100, 200, and 250 °C. (b) ε_r–E curves measured at 25 and 250 °C for the same nanocapacitor as Figure 3a. Frequency was 10 kHz. The data of $Ba_{0.5}Sr_{0.5}TiO_3$ (25 °C, t = 24 nm)[19] are also included for a comparison. (c) Temperature dependence of the capacitance change relative to RT value ($\Delta C/C_{RT}$) for $Ca_2Nb_3O_{10}$ nanosheet and perovskite thin films.[9,10,18] (d) Plot of the temperature coefficients (τ) for $Ca_2Nb_3O_{10}$ nanosheet and high-κ thin films.[9,10,18]

boundaries between the nanosheets (i.e., $SrRuO_3$ substrate). I–V curves were obtained at various positions (Figure 2b). The onset of current flow occurred when the potential of the Rh cantilever was above +2.1 V and below −1.5 V. This gap of 3.6 V corresponds roughly to the bandgap energy (3.44 eV) of $Ca_2Nb_3O_{10}$ nanosheet.[17] We note that such insulating properties were stable even at 200 °C. As was evident from Figure 2e–h, there was no noticeable change in 2D morphology and insulating response at 100 and 200 °C. Such a superior thermal stability was not specific to substrate choice and interface geometry; almost identical results were obtained from a Pt substrate with Au and Pt cantilevers. Thus, observed thermal stability is materials property inherent from $Ca_2Nb_3O_{10}$ nanosheet. Our previous structural studies revealed that the crystallization/nucleation is severely hindered in 2D perovskite nanosheets; the perovskite-type nanosheet was stable up to 800 °C.[14] Such a 2D bound reactant provides an unusual environment in structure reconstruction, causing a robust thermal stability. High thermal robustness was also confirmed in current samples; XRD pattern appeared to remain virtually unchanged up to 200 °C (the temperature range for this *in situ* study) (see Figure S1 in the Supporting Information). In $Ca_2Nb_3O_{10}$ nanosheet, 2D nature is also advantageous for dielectric applications. Due to quantum confinement effects, 2D nanosheets have an enlarged bandgap, causing a highly insulating nature compared to bulk systems.

For dielectric characterization, we used Au/$(Ca_2Nb_3O_{10})_n$/$SrRuO_3$ nanocapacitors with n = 10 (Figure 1d). By engineering dielectric/electrode interfaces using LB assembly, we fabricated an ideal metal–insulator–metal structure with an atomically sharp and clean interface, realizing the full potential of high-κ nanosheets. Such highly organized nanocapacitors exhibited stable dielectric performance over a wide temperature range.

Figure 3a shows the frequency dependence of the ε_r of an Au/$(Ca_2Nb_3O_{10})_n$/$SrRuO_3$ (n = 10) nanocapacitor at 25, 100, 200, and 250 °C. The nanocapacitors measured at RT showed a stable dielectric response; the ε_r value was 206 at 10 kHz, which almost agrees with that of our previous reports.[12] The ε_r value exhibited a rather flat frequency dispersion in the regime of 500 Hz ∼ 2 MHz; the dielectric loss values (tan δ) are in the range of 2–4%. These superior high-κ properties of $Ca_2Nb_3O_{10}$ nanosheet also showed a minimal variation as a function of temperature. With increasing temperature, the dielectric response was slightly degraded, but the ε_r value still kept a high level (∼200) even at 250 °C. Figure 3b shows the electric-field dependence of the ε_r for the same nanocapacitor at 25 and 250 °C. The data of $Ba_{1-x}Sr_xTiO_3$ with a comparable thickness (t = 24 nm) are also included for a comparison.[18] The ε_r–E curves showed a typical paraelectric behavior; no hysteresis was observed when the applied electric field scanned from positive to negative bias. A stable dielectric response was obtained even in a high electrical field extending up to ∼2 MV/cm. This behavior is in contrast to that of $Ba_{1-x}Sr_xTiO_3$ where the capacitance is reduced by 50% between 0 and 2 MV/cm.[18,19] These results suggest a good dielectric stability of $Ca_2Nb_3O_{10}$ nanosheet against temperature and electric field. Figure 3c compares the temperature dependence of the capacitance values for $Ca_2Nb_3O_{10}$ nanosheet and perovskite thin films. Figure 3d summarizes the temperature coefficients (τ) for $Ca_2Nb_3O_{10}$ nanosheet and various high-κ thin films.[9,10,18] Clearly, $Ca_2Nb_3O_{10}$ nanosheet exhibited a robust thermal

stability over a wide temperature range (−50−250 °C); the capacitance variation was about −5.5%. The τ was −180 ppm/K, which is much smaller than typical high-κ dielectrics (>−1000 ppm/K for $Ba_{1-x}Sr_xTiO_3$)[10,18,20] (Figure 3d). We note that even with an extremely small thickness of ∼15 nm, nanosheet-based capacitor shows a small τ value, which is almost comparable to the best τ value (+110 ppm/K for $CaBi_4Ti_4O_{15}$)[9] in the literatures.

Figure 4 depicts the leakage current density versus electric field (J−E) curves at 25, 100, 200, and 250 °C for the Au/$(Ca_2Nb_3O_{10})_n$/$SrRuO_3$ (n = 10) nanocapacitor. For RT, $Ca_2Nb_3O_{10}$ nanosheet showed a highly insulating nature; the J value was of an order of 10^{-7} A/cm^2 at +100 kV/cm, which almost agrees with that of our previous reports.[12] $Ca_2Nb_3O_{10}$ nanosheet also exhibited a strong dielectric endurance in a high electrical field; a dielectric breakdown occurred at ∼3.5 MV/cm. Such superior insulating properties were stable up to 250 °C. $Ca_2Nb_3O_{10}$ nanosheet exhibited a modest temperature dependence with a slight increased J value at elevated temperatures. The J value at 250 °C still kept a low leakage level of 1×10^{-6} A/cm^2 at +100 kV/cm, which is 2 orders of magnitude smaller than that of $Ba_{1-x}Sr_xTiO_3$.[10,18]

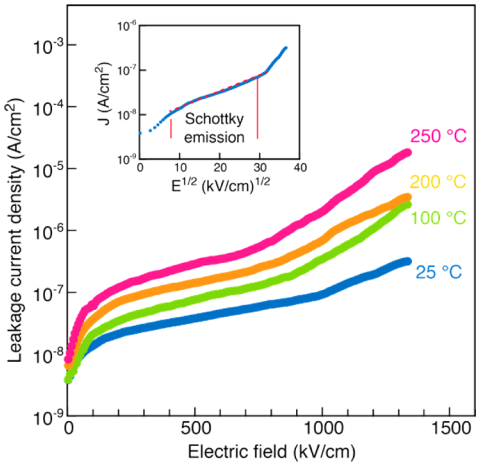

Figure 4. J−E curves measured at 25, 100, 200, and 250 °C for an Au/$(Ca_2Nb_3O_{10})_n$/$SrRuO_3$ (n = 10) nanocapacitor. Inset shows ln J−$E^{1/2}$ plot for the J curve at 25 °C.

In the Au/$(Ca_2Nb_3O_{10})_n$/$SrRuO_3$ nanocapacitors, the leakage current property is governed by a Schottky-type barrier; a contact between n-type nanosheet film and Au with a high work function, which allows the electrons to flow from the film into the electrode. We assume that 2D nanosheets with a large bandgap effectively blocks the current conduction, compared with bulk perovskites. In this context, we note that ln$J$−$E^{1/2}$ plots show a large plateau behavior at the middle E range [10−30 (kV/cm)$^{1/2}$], which corresponds to the Schottky current conduction mechanism (Figure 4 inset). Clearly, the J−E profiles can be well fitted by the corresponding ln J−$E^{1/2}$ plots. At high temperatures, there still existed a plateau but the region was slightly smaller than that of the RT case. This is probably due to the change in current modes. With increasing the electric field at high temperatures, other high current conduction mechanisms such as Poole-Frenkel and/or thermal-activation effects also contribute to leakage currents.

These results indicate that $Ca_2Nb_3O_{10}$ nanosheet is a useful candidate for high-temperature capacitor materials. From a practical viewpoint, thin-film geometries are critical for optimal efficiency with high storage density. In typical perovskite thin films such as $BaTiO_3$ and $Ba_{1-x}Sr_xTiO_3$, however, strong size-dependent effects arise as the film thickness is reduced down to several nanometers.[21−23] This size effect unambiguously worsens their potential functionalities by suppressing dielectric responses and raising leakage current. In this context, $Ca_2Nb_3O_{10}$ nanosheet is quite unique; the high ε_r values persist even in <10 nm, which is in sharp contrast to the size-induced dielectric collapse in typical perovskite thin films. In the ultrathin region (<20 nm), the ε_r value (∼200) of $Ca_2Nb_3O_{10}$ nanosheets is larger than those of the other perovskites (with ε_r < 100). Additionally, thermally stable high-κ response was maintained even in the thinner films with n = 3, 5 (see Figure S2 in the Supporting Information), a property being almost comparable to the size-effect free characteristic observed at room temperature.[12] Perovskite nanosheets thus constitute the highest-κ dielectrics ever realized in perovskite nanofilms and may be the key to ultrascaled capacitor devices. The simultaneous improvement of ε_r with small τ and low J values in high-κ nanodielectrics is quite unique, in marked contrast to those observed in typical perovskite dielectrics, where the τ values are generally larger in higher ε_r materials (Figure 3d)

Perovskite nanosheets also offer a unique opportunity for tailoring the dielectric properties through doping and lattice engineering. We previously reported that in $Ca_2Nb_3O_{10}$ nanosheets, A-site modification with Sr^{2+} ions enhances the ε_r value, whereas B-site modification with Ta^{5+} ions improves the leakage current.[24] Perovskite nanosheets also enable control over the temperature dependence. Our preliminary study revealed the overall trend of τ from negative values (−210 ppm/K) at Ca-based nanosheets ($Ca_2Ta_3O_{10}$) to positive values (+150, +180 ppm/K) at Sr-based nanosheets ($Sr_2Nb_3O_{10}$, $Sr_2Ta_3O_{10}$) in the temperature range (−25 ∼ +150 °C). The opposite signs of Ca- and Sr-based nanosheets offers the tantalizing possibility that solid solutions could be formed with high ε_r value with near-zero τ. Together with these aspects, perovskite nanosheets have great potential for a rational design and construction of high-temperature capacitor devices.

In summary, we investigated high-temperature dielectric responses of 2D $Ca_2Nb_3O_{10}$ nanosheet with a paraelectric ground. Through *in situ* characterizations, we found a robust thermal stability of $Ca_2Nb_3O_{10}$ nanosheet even in a monolayer form, and layer-by-layer assembled nanocapacitors exhibited stable dielectric responses up to 250 °C. These results indicate that $Ca_2Nb_3O_{10}$ nanosheet is an important candidate for high-temperature capacitor materials. Nanosheet-based nanocapacitors retained the size-free high-ε_r characteristic and high insulation resistance with high breakdown voltages at high temperatures up to 250 °C. They also exhibited small τ value, offering a superior performance over existing X8R or X9R technologies. In this study, we discussed the temperature stability up to 250 °C. However, because $Ca_2Nb_3O_{10}$ nanosheet itself possess a robust structural stability up to 700 °C, the optimization of device structures would facilitate to use much higher temperatures (even at 500 °C). In addition, perovskite nanosheets are Pb-Free and RoHS compliant without the need of any exemptions, which are a key issue for future electronics.

■ ASSOCIATED CONTENT

Supporting Information

Experimental details on nanosheet synthesis, film fabrication, and characterization. Structural characterization by XRD. Thickness dependence of the dielectric response. This material is available free of charge via the Internet at http://pubs.acs.org.

■ AUTHOR INFORMATION

Corresponding Author

*E-mail: osada.minoru@nims.go.jp.

Author Contributions

The manuscript was written through contributions of all authors.

Notes

The authors declare no competing financial interest.

■ ACKNOWLEDGMENTS

This work was partly supported by a Grant-in-Aid for Construction of the World Premier Research Institute (WPI Initiative in Materials Nanoarchitectonics), MEXT, CREST, JST, and the Grand-in-Aid for Scientific Research, JSPS, Japan.

■ REFERENCES

(1) Hammoud, A. N.; Myers, I. T. Evaluation of High Temperature Capacitor Dielectrics. *Annu. Rep. Conf. Electr. Insul. Dielectr. Phenom.* **1989**, 459−464.

(2) Johnson, R. W.; Evans, J. L.; Jacobsen, P.; Thompson, J. R.; Christopher, M. The Changing Automotive Environment: High-Temperature Electronics. *IEEE Trans. Electron. Packag. Manuf.* **2004**, *27*, 164−176.

(3) Randall, C. A.; Ogihara, H.; Kim, J.-R.; Yang, G.-Y.; Stringer, C. S.; Trolier-McKinstry, S.; Lanagan, M. High Temperature and High Energy Density Dielectric Materials. *IEEE Int. Pulsed Power Conf. Proc.* **2009**, 346−351.

(4) Hennings, D.; Schnell, A.; Simon, G. Diffuse Ferroelectric Phase Transitions in $Ba(Ti_{1-y}Zr_y)O_3$ Ceramics. *J. Am. Ceram. Soc.* **1982**, *65*, 539−544.

(5) Kishi, H.; Mizuno, Y.; Chazono, H. Base-Metal Electrode-Multilayer Ceramic Capacitors: Past, Present and Future Perspectives. *Jpn. J. Appl. Phys.* **2003**, *42*, 1−15.

(6) Wei, X. Y.; Feng, Y. J.; Yao, X. Dielectric Relaxation Behavior in Barium Stannate Titanate Ferroelectric Ceramics with Diffused Phase Transition. *Appl. Phys. Lett.* **2003**, *83*, 2031−2033.

(7) Lim, J. B.; Zhang, S.; Kim, N.; Shrout, T. R. High-Temperature Dielectrics in the $BiScO_3$−$BaTiO_3$−$(K_{1/2}Bi_{1/2})TiO_3$ Ternary System. *J. Am. Ceram. Soc.* **2009**, *92*, 679−682.

(8) Dittmer, R.; Jo, W.; Damjanovic, D.; Rödel, J. Lead-Free High-Temperature Dielectrics with Wide Operational Range. *J. Appl. Phys.* **2011**, *109*, 034107.

(9) Takahashi, K.; Suzuki, M.; Kojima, T.; Watanabe, T.; Sakashita, Y.; Kato, K.; Sakata, O.; Sumitani, K.; Funakubo, H. Thickness Dependence of Dielectric Properties in Bismuth Layer-Structured Dielectrics. *Appl. Phys. Lett.* **2006**, *89*, 082901.

(10) Kimura, J.; Takuwa, I.; Matsushima, M.; Yasui, S.; Yamada, T.; Funakubo, H. Temperature and Electric Field Stabilities of Dielectric and Insulating Properties for *c*-Axis-Oriented $CaBi_4Ti_4O_{15}$ Films. *J. Appl. Phys.* **2013**, *114*, 027002.

(11) Osada, M.; Sasaki, T. Two-Dimensional Dielectric Nanosheets: Novel Nanoelectronics from Nanocrystal Building Blocks. *Adv. Mater.* **2012**, *24*, 210−228.

(12) Osada, M.; Akatsuka, K.; Ebina, Y.; Funakubo, H.; Ono, K.; Takada, K.; Sasaki, T. Robust High-κ Response in Molecularly Thin Perovskite Nanosheets. *ACS Nano* **2010**, *4*, 5225−5232.

(13) Wang, C.; Osada, M.; Ebina, Y.; Li, B.-W.; Akatsuka, K.; Fukuda, K.; Sugimoto, W.; Ma, R.; Sasaki, T. All-Nanosheet Ultrathin Capacitors Assembled Layer-by-Layer *via* Solution-Based Processes. *ACS Nano* **2014**, *8*, 2658−2666.

(14) Li, B.-W.; Osada, M.; Ebina, Y.; Akatsuka, K.; Fukuda, K.; Sasaki, T. High Thermal Robustness of Molecularly Thin Perovskite Nanosheets and Implications for Superior Dielectric Properties. *ACS Nano* **2014**, *8*, 5449−5461.

(15) Ebina, Y.; Sasaki, T.; Watanabe, M. Study on Exfoliation of Layered Perovskite-Type Niobates. *Solid State Ionics* **2002**, *151*, 177−182.

(16) Li, B.-W.; Osada, M.; Ozawa, T. C.; Ebina, Y.; Akatsuka, K.; Ma, R.; Funakubo, H.; Sasaki, T. Engineered Interfaces of Artificial Perovskite Oxide Superlattices *via* Nanosheet Deposition Process. *ACS Nano* **2010**, *4*, 6673−6680.

(17) Akatsuka, K.; Takanashi, G.; Ebina, Y.; Haga, M.; Sasaki, T. Electronic Band Structure of Exfoliated Titanium- and/or Niobium-Based Oxide Nanosheets Probed by Electrochemical and Photoelectrochemical Measurements. *J. Phys. Chem. C* **2012**, *116*, 12426−12433.

(18) Parker, C. B.; Maria, J.-P.; Kingon, A. I. Temperature and Thickness Dependent Permittivity of $(Ba,Sr)TiO_3$ Thin Films. *Appl. Phys. Lett.* **2002**, *81*, 340−342.

(19) Padmini, P.; Taylor, T. R.; Lefevre, M. J.; Nagra, A. S.; York, R. A.; Speck, J. S. Realization of High Tunability Barium Strontium Titanate Thin Films by RF Magnetron Sputtering. *Appl. Phys. Lett.* **1999**, *75*, 3186−3188.

(20) Cava, R. J. Dielectric Materials for Applications in Microwave Communications. *J. Mater. Chem.* **2001**, *11*, 54−62.

(21) Hwang, C. S. Thickness-Dependent Dielectric Constants of $(Ba,Sr)TiO_3$ Thin Films with Pt or Conducting Oxide Electrodes. *J. Appl. Phys.* **2002**, *92*, 432−437.

(22) Stengel, M.; Spaldin, N. A. Origin of the Dielectric Dead Layer in Nanoscale Capacitors. *Nature* **2006**, *443*, 679−682.

(23) Chang, L.-W.; Alexe, M.; Scott, J. F.; Gregg, J. M. Settling the "Dead Layer" Debate in Nanoscale Capacitors. *Adv. Mater.* **2009**, *21*, 4911−4914.

(24) Osada, M.; Sasaki, T. *A*- and *B*-Site Modified Perovskite Nanosheets and Their Integrations into High-*k* Dielectric Thin Films. *Int. J. Appl. Ceram. Technol.* **2012**, *9*, 29−36.